Uncovering ecological associations by learning latent representations of species responses and effects from their co-distribution

Sara Si-moussi, Esther Galbrun, Mickael Hedde, Wilfried Thuiller

October 5, 2019

1 Background

To understand the drivers of species distribution and their abundance is an age-old question in biogeography (von Humboldt 1805). Niche theory explains the geographical dynamics of species by a set of properties and adaptive behaviors they exhibit that allows them to thrive in specific conditions and decline in others (Chase and Leibold 2003, Peterson 2011). The ranges of abiotic variables, such as climate and soil characteristics, that match the ecophysiological requirements of a species delimit its potential habitats (Grinnellian niche, Grinnell 1917) or (Fundamental niche, Hutchinson 1957) at a macro scale. Habitat suitability models or species distribution models (SDMs) aim to infer this niche by establishing statistical relationships between observed presences (realized niche) and the environmental characteristics of the corresponding locations (Hirzel 2008).

SDMs have proven useful to predict species ranges in response to climate change, providing operational tools to conservation biologists (Guisan and Thuiller 2005, Elith 2006). However, they predict multiple species distributions separately hence ignoring possible dependencies that could restrain or extend species' ranges from what is expected with the sole consideration of abiotic factors. Indeed, species may exclude one another locally (competitive exclusion, Gause 1934) or differentiate each other's areas and resources (niche partitioning, Schoner 1974). Conversely, some species facilitate others by modifying the environment in a way that creates habitats or enables access to resources for other species (engineering, facilitation, Boucher 1982). Although these interactions take place at a local scale, some of them may scale up to restricting the range of the species. Thus, the inability to take into account the presence or absence of other species is an important source of underfitting for SDMs (Wisz 2013).

Over the last decade, several approaches have been proposed to infer interspecific associations within the latter models by jointly analyzing the co-distribution of multiple species. This led to the development of Joint Species Distribution Models (Pollock et al. 2014). The gist is that once we have accounted for abiotic factors, the unexplained variance is attributed to the effect of species on one another, typically captured by the residuals' correlation matrix. As they rely purely on correlation, JSDMs are limited to inferring symmetric associations between species; such as mutualism and competition. Asymmetric interactions; such as commensalism, amensalism and predation; are therefore inherently out of reach for these models. (Lany et al 2018) proposed a JSDM that allows to capture asymmetric associations but it requires access to longitudinal data.

Another research field that is also concerned with inferring associations from co-occurrence is natural language processing (NLP). NLP modelers try to understand semantic associations between words on the basis of the contexts they appear in. The context of a word is the list of words around it in a sentence. A state of art method in this area is word2vec (Mikolov et al 2013). Word2vec learns distributed representations for words in the form of dense vectors called embeddings. The embedding of a word captures information about other words it co-occurs with. The probability of a word occurring in a particular sentence of a text depends on the word's semantic compatibility with other words occurring in that sentence. Word embeddings, such as word2vec, aim to learn multidimensional representations of words that captures this contextual semantic compatibility. By analogy, in community ecology, the probability of the presence of a species in a given abiotically suitable site depends on its compatibility with every other species in the observed community.

(Rudolph et al 2016) introduced a generalization of word embeddings to any type of data following an exponential family distribution, including binary and ordinal data, called exponential family embeddings. Building on the previous work, we propose a conditional probabilistic model of species co-distributions that can be trained jointly with any habitat suitability model on presence/absence or count data to infer interspecific associations. We evaluate the potential of the model to recover correct associations on empirically observed as well as simulated communities.

2 Material and Methods

Species live where three main conditions are satisfied. First, the location has to be accessible from its biogeographic origins. This relates to the dispersal capacity of the species and the presence of migration opportunities or barriers. Second, the species shall find appropriate abiotic conditions to grow and maintain its population. This condition is referred to as *habitat suitability* and is the target of Habitat Suitability Models. Third, the species population density within communities is also influenced by intraspecific and interspecific interactions, which could alter potentially the range of the species as well as its local abundance (Guisan, Thuiller, Zimmermann 2017). Although we recognize the importance of dispersal and spatial processes, we will emphasize the last two requirements in this study.

2.1 Key concepts and assumptions

In what follows, we introduce key concepts used in the inference model.

2.1.1 Responses, effects and biogeographical associations

A *biogeographical association* describes the relative influence of a pair of species on one another's abundances. This influence can be stronger or of different type (positive, negative or neutral) from one side to the other. An association represents a consistent pattern in co-occurrence with potentially multiple mechanistic explanations: direct biotic interaction, indirect interaction through the environment or a shared correlation to an unmeasured environmental variable or an unobserved group of organisms.

Concretely, we define the association $\mathcal{A}(a, b)$ involving species (a, b) with the tuple $(\mathcal{A}_{ab}, \mathcal{A}_{ba})$ representing the *association strength* on b and a respectively. Specifically, $\mathcal{A}_{ab}$ represents the change (excess if positive, deficit if negative, none if null) in *target* species b's abundance induced by the presence of an individual from *source* species a.

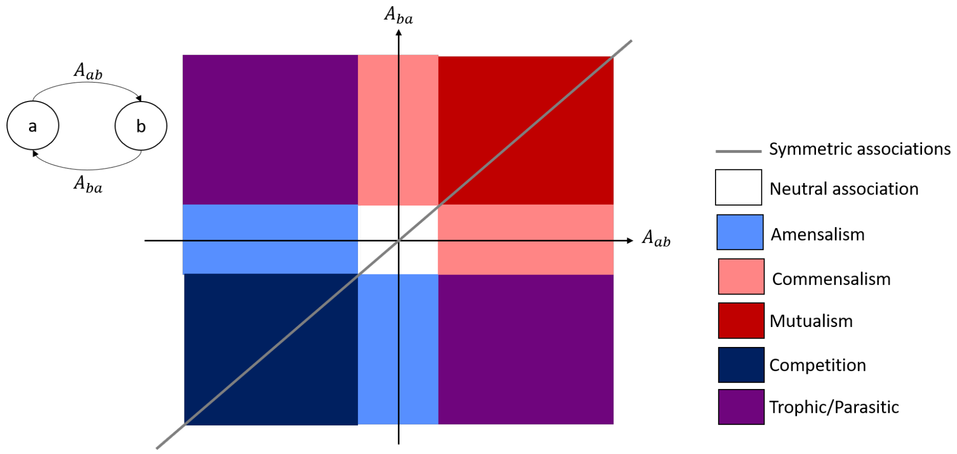

Figure 1: Mapping pairwise association strengths to potential interaction classes. The first bissector represents the association domain covered by correlation-based approaches including Joint Species Distribution Models.

The association strength depends on two latent parameters: the *effect* applied by the source and the *response* of the target. We assume these parameters are controlled by intrinsic traits of the species, encoded in two separate real vectors referred to as embeddings. The effect captures the type of organisms the species allows when it is presente . Whereas the response controls the type of biotic contexts the species would strive in. For instance, trees with spreading canopy create shade (effect) that selects only shade-tolerant (response) species and exclude others.

We note the response of species a: ρ_a and its effect: α_a, both d-dimensional real-valued vectors. In practice, d is significantly smaller than half the number of species. We stack response and effect embeddings of modeled species rowwisely in separate matrices ρ and α. We encode pairwise associations in a square asymetric matrix such that rows and columns are the modeled species. Each cell represents the strength directed from the row to the column species. The association matrix is then written as:

$$\mathcal{A} = \rho \times \alpha$$

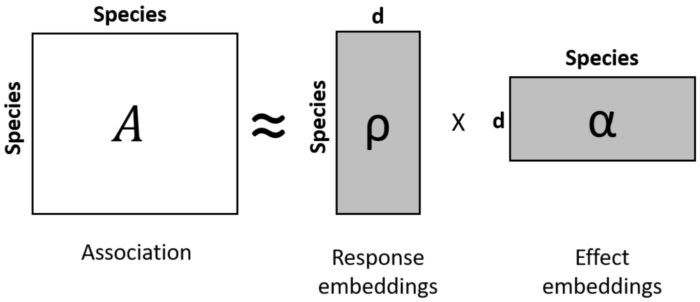

Figure 2: Association matrix factorization.

Note that species with similar response embeddings, *response groups*, represent row-wise clusters in the association matrix. Conversely, species with similar effect embeddings, *effect groups*, represent column-wise clusters in the association matrix. The overlap of both groups forms *structural roles* in the association network which adjacency matrix is $\mathcal{A}$.

2.1.2 Biotic context

The *biotic context* encodes our assumptions about *potential* biotic effects a *target* species is exposed to in a given *location*. In the simplest case, without any prior knowledge, it is formed of individuals from other species observed in the same location. Specifically, the biotic context of the j^{th} species in the i^{th} site, noted $c_{i,j}$, is computed as follow:

$$c_{i,j} = \{k \mid k \neq j, y_{i,k} > 0\}$$

We obtain the aggregated effect of the biotic context by averaging the effects embeddings of its elements weighted by their respective abundances:

$$z_{i,j} = \frac{1}{|c_{i,j}|} \sum_{k \in c_{i,j}} y_{i,k} \cdot \alpha_k$$

This formulation allows the compensation between the presence of facilitators and competitors. By weighting with abundance, we consider implicitely that individuals from the same taxa are similar and contribute equally to the community structure. Conversely, the effect of rare taxa would only be apparent if their per capita effect is stronger than the aggregated effect of dominant groups.

The biotic context carries implicit constraints on the structure of species association networks by restricting the set of potential associations a priori. We illustrate some alternative definitions of the biotic context with their data/knowledge requirements and relevant effect aggregation functions in Appendix.

2.2 A conditional probabilistic model of abundance

2.2.1 Notation

The abundance of the j^{th} taxa on the i^{th} site is noted $y_{i,j}$. The abiotic environment in the i^{th} site, noted E_i, is described by the abiotic feature vector X_i computed by the feature extraction model $\mathcal{F}$.

2.2.2 Conditional generative model of abundance

The abiotic suitability score of S_i for T_j, noted $e_{i,j}$, is given by a habitat suitability model $\mathcal{H}$ fitted on the target taxa's occurrences.

$$X_i = \mathcal{F}(E_i)$$

$$e_{i,j} \sim \mathcal{B}(\mathcal{H}_j(X_i))$$

On locations where the abiotic environment is not suitable, the probability mass of the species abundance is concentrated on zero. Otherwise, the abundance is a function of its biotic context.

Following (Rudolph et al 2016), we formulate the model using the canonical form of the exponential family $\mathcal{E}$ where the natural parameter depends on the response ρ_j of the target taxa and the biotic context effect $z_{i,j}$. An offset is used to represent the baseline abundance for each taxa in the event of an empty biotic context. A link function f is used to scale the outcome back to the domain of the target variable.

$$y_{i,j} \sim \begin{cases} \mathcal{E}(\eta_{i,j}, \tau_{i,j}) & \text{if } e_{i,j} = 1, \\ \delta_0 & \text{otherwise.} \end{cases}$$

$$\eta_{i,j} = f(\rho_j \cdot z_{i,j} + o_j)$$

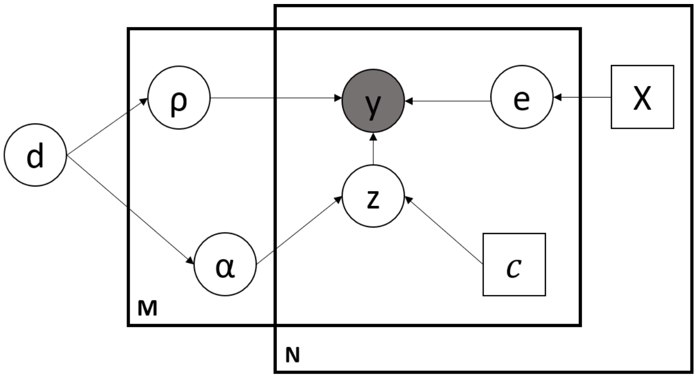

Figure 3: Plate diagram of the generative model of abundance.

Distribution	**Link function**	**Parameter mapping**
Bernoulli	Identity	$p_{i,j} = \sigma(\sum_{k \in c_{i,j}} y_{i,k}\mathcal{A}_{j,k} + o_j)$
Poisson	Identity	$\lambda_{i,j} = \exp(\sum_{k \in c_{i,j}} y_{i,k}\mathcal{A}_{j,k} + o_j)$
Poisson	log	$\lambda_{i,j} = \sum_{k \in c_{i,j}} y_{i,k}\mathcal{A}_{j,k} + o_j$
Neg binomial	Identity	$p_{i,j} = \exp(\sum_{k \in c_{i,j}} y_{i,k}\mathcal{A}_{j,k} + o_j)$

Table 1: Parameter mapping and link function choices for common distributions

A direct consequence of this choice of representation is that we can write the mean abundance as an aggregation of pairwise association strengths.

$$\eta_{i,j} = f(\sum_{k \in c_{i,j}} y_{i,k}\mathcal{A}_{j,k} + o_j)$$

We provide in Table 1 the expressions of the natural parameter, the suffiscient statistic and the likelihood in the special cases where $\mathcal{E}$ is a binomial, poisson and negative binomial distribution with known number of failures.

2.2.3 Inference

We consider a dataset $\mathcal{D} = \{X, Y\}$ of observed abundances Y of m species and measured or computed features X. We compute the sets of positive (present species) and negative (absent species) examples on each site i:

$$\mathcal{S}_i^+ = \{j \in [1, m] \mid y_{ij} > 0\}$$
$$\mathcal{S}_i^- = \{j \in [1, m] \mid y_{ij} = 0\}$$

We minimize the log-likelihood of the observed abundances on each site for all positive examples. As negative examples are much more numerous than positive ones, we down-weight their importance by selecting a random subsample of $r\%$ of them. By introducing noisiness into the objective function, this

Parameters	Hyperparameters
$\Theta = \{\rho, \alpha, \theta_{HSM}\}$	$\Phi = \{d, O, \lambda\}$
ρ: response embeddings matrix. α: effect embeddings matrix. θ_{HSM}: Habitat suitability model parameters.	d: embedding dimension. O: vector of species offsets. λ: regularization coefficient. r: negative subsample rate.

Table 2: Summary of parameters and hyperparameters.

technique increases robustness of the estimations and prevents overfitting. To promote smaller embeddings and sparse resulting association matrices, we add lasso penalties on the embedding vectors.

In summary, given a choice of hyperparameters Φ (see Table 2 for summary), the inference aims to infer the value of the parameters Θ that minimizes the objective function $\mathcal{L}$. To do so, we use online stochastic gradient descent. We provide the detailed objective equation and its derivative with respect to each parameter in the supporting materials.

2.3 Validation on simulated data

We used a process-based stochastic model adapted from Virtualcomm (Gallien and Münkemüller 2015) to simulate the assembly of individuals from a regional species pool into communities, on different locations sampled along an environmental gradient. The assembly process is controlled by three filtering mechanisms: the response to the abiotic environment, the outcome of biotic interactions and reproduction. For simplicity, the spatial structure of communities and thus dispersal processes are ignored. In other words, there is no exchange of individuals between neighboring communities.

The simulation starts with a given or random initial composition for each community independently. Individuals are replaced through time until an equilibrium state is reached or a user-defined number of iterations is completed. The final communities' composition is returned at the end.

2.3.1 Simulation experiment

We evaluate the ability of the proposed model to recover interspecific interactions without supervision from simulated datasets of known interactions. We set up an experiment similar to (Pollock et al, in prep) where multiple simulations are run on 500 random points on a gradient between 0 and 100 with different configurations of the prior interaction matrix. Specifically, four configuration modes were tested: absence of interaction, positive interactions only, negative interactions only and both positive and negative interactions. In each mode, we varied the number of species (5, 10 or 20), the number of interacting pairs (sparse, dense) and whether the interaction matrix includes asymmetric effects. Positive (resp. negative) effects were all set to 1 (resp. minus 1) as we were interested in the nature or sign of the interactions rather than their strengths. The full-factorial design of this experiment produced 29 simulation datasets, summarized in Figure 4).

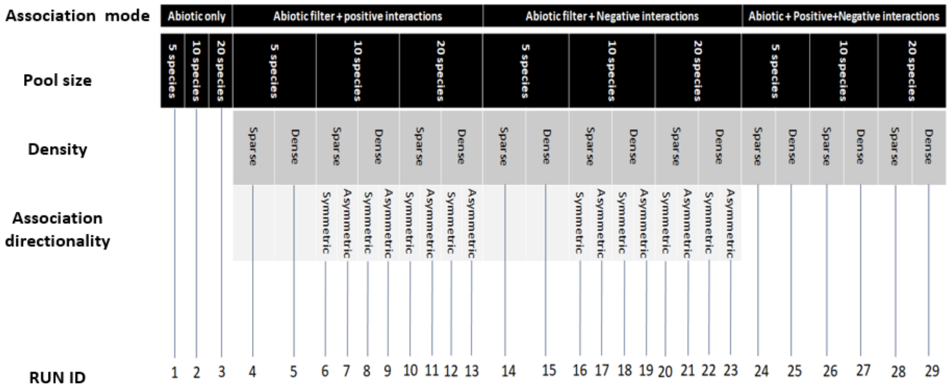

Figure 4: Design of the simulation experiment.

2.3.2 Simulation diagnosis and inference complexity

As a proxy for the complexity of the inference problem and a simulation diagnosis tool, we evaluate the degree by which the observed patterns of species dependencies in the final communities strongly reflect the simulation parameters. To do that, for a pair of source s and target t species, we compute two indices that quantify the geographic overlap and the relative variation in abundance.

Co-occurrence index It is a symmetric index. It measures the geographic overlap of the species distributions. In particular, we use the jaccard set similarity measure to compute it.

$$J_{s,t} = J_{t,s} = \frac{|S_i \mid y_{i,s} > 0 \wedge y_{i,t} > 0|}{|S_i \mid y_{i,s} > 0 \vee y_{i,t} > 0|}$$

- A value of $J_{s,t}$ close to 1 indicates high geographic overlap.
- A value close to 0 indicates geographic separation.
- A value around 0.5 could indicate average overlap, no conclusion can be made out of it.

Geographic relative effect on abundance index The GREA index is asymetric. It measures the relative increase in the target species' abundance when the source species is present.

$$E_{s,t} = \{y_{i,t} - \bar{y}_t \mid (Y_{i,s} > 0)\}$$

$$R_{s,t} = mean(E_{s,t}) \pm 1.96 \cdot stddev(E_{s,t})$$

- If the interval does not contain zero then the observed dependencies translate a distinct effect type.
- The greater the standard deviation, the higher the uncertainty on the effect strength.
- An interval which contains zero indicates conflicting effect types, often due to confounding effects of other species or a neutral association if the mean is close to zero.

2.3.3 Training

On each dataset, we count the number of individuals for each species in each location to produce the abundance dataset. Then, we binarize the counts to produce the site by species occurrence matrix.

We model the abiotic response of the species using independent Generalized Linear Models with logistic links and one quadratic term. This model predicts the Habitat Suitability of a location for a target species given its associated environmental value.

We apply the proposed association inference model with a negative binomial distribution to fit the species counts. We set the offsets for each species as the average value of its abundance on its sites of presence. We also add Lasso penalties with $\lambda = 0.01$ on response and effect embeddings to promote the sparsity of their products.

To select the embeddings' dimension d, we use a 5-fold cross-validation scheme where we monitor the deviance of the predicted abundances. With the selected dimension d, we train the model on 1000 bootstrap samples from the training set and we evaluate its performance on an independent test set using two metrics: Area Under the Curve of the HSM component's predicted probabilities of presence and the deviance of predicted abundances on positive examples. Finally, we compute the 95% confidence interval of the inferred association matrix's mean.

2.3.4 Association filtering

We build the significative association matrix in two steps: statistical filtering and biogeographical filtering. In statistical filtering, we set to zero all associations which confidence interval contains zero and we keep the mean value for the rest. The biogeographical filtering aims to further eliminate associations that could be true given the latent representations of the species. However, they are unlikely to have generated the observed dataset as they are inconsistent with some biogeographical constraints.

For instance, facilitation between two species requires co-existence. Thus, we set to zero any inferred positive effect involving two non-co-occurring species (Sanderson, Pimm et al 2015). On the other hand, competition does not require co-occurrence and may even explain the absence of it. In this case, we assume that negatively associated species should at least live in similar environments for us to consider a potential association. Concretely, we compute the ranges of the environmental values corresponding to their observed points of presence. We retain negative associations among pairs with overlapping environmental ranges or significant similarity (greater than a user-defined threshold) of their habitat suitability parameters, translating akin habitat preferences.

2.3.5 Validation metrics

We formulate an edge classification problem on the fully connected species association network. The problem consists of finding a mapping f_A from any edge (source species, target species) to one of the three effect classes: negative, positive, neutral. Let the pair $(A, \hat{A})$ be composed of the simulated, respectively the inferred, association matrices. We define the true mapping f_A as follow:

$$f_A : (S_i, S_j) \mapsto \begin{cases} \textit{positive} & \text{if } A_{i,j} > 0, \\ \textit{negative} & \text{if } A_{i,j} < 0, \\ \textit{neutral} & \text{otherwise.} \end{cases}$$

We compute the predicted mapping $f_{\hat{A}}$ similarly using $\hat{A}$ instead of A. Finally, we compute the multi-class performance metrics (recall, precision, f1-score) for the predicted classes using the simulation association classes as a reference. (Table 3)

2.4 Evaluation on empirical data

In this part, our objective is to evaluate the ability of the model to recover meaningful associations from empirical observations of species abundances. To do that, we use the plant dataset described in (Choler et al. 2005).

2.4.1 Data description

The data describes the counts of 84 plant species, collected in July 2000 on 75 units distributed along a mesotopographical gradient. Each unit is of size 5×5 m. It is associated to a set of numeric environmental features: the slope inclination in degrees at its location (Slope), the average snowmelt date in julian days between 1997-1999 (Snow), the percentage of non vegetated soil due to physical processes (PhysD) and that due to marmot activity ZoogD. In addition to that, the relative south aspect (Aspect) and the microtopographic landform index (Form) were documented at each location.

2.4.2 Preprocessing

We apply a one-hot encoding scheme to the categorical features Aspect and Form and we scale the numerical features. For each plant species, we pretrain an independent generalized linear model with a logit link to predict its occurrences using the preprocessed environmental features as inputs. We use the learnt weights as initial parameter values in the habitat suitability component of our model.

We define the biotic context for a target species as the set of plants observed on the location of interest. We use a negative binomial distribution to fit the plants' counts jointly as a function of their respective biotic contexts. We also add an L1 penalty on the embedding vectors' norms to the global likelihood to promote the sparsity of the resulting association matrix. We set the initial value of the embedding vectors using random samples from a uniform distribution on the [-0.01,0.01] interval. Finally, the offset value for each species was set to its average count on occurrence points.

2.4.3 Training configuration

We use a multi-label stratified scheme (using the skmultilearn library) to split the observations into training and test sets while ensuring that all species are covered and their proportions are preserved in both sets.

We proceed to training the full model using Stochastic Gradient Descent (learning rate=0.01, momentum=0.8) on the counts training dataset with a negative examples subsampling rate of 25%. We monitor the negative log-likelihood of positive examples (presences) on the validation set after each full pass of the training set to assess the convergence of the training. We stop when the loss stops decreasing or when 200 epochs have elapsed.

2.4.4 Hyperparameter search and model selection

For a species pool size m, we select the embedding dimension search space on the set of powers of 2 below $m/2$ (to improve hyperparameter search speed). In our case, with $m = 82$, values of the embedding dimension K are chosen from the set $\{2, 4, 8, 16, 32\}$.

As we increase the value of the L1 penalty parameter λ, some components of the embedding vectors take extremely small values for all species (below $\epsilon = 10^{(} - 5))$. In this case, these components have no effect on the computed associations. By removing them, the embeddings shrink to a smaller effective dimension K' equal to the number of retained components. Very high values of λ lead to $K' = 0$, resulting in a zero association matrix. In the latter case, the interaction model is only parameterized by the species offset counts.

For each value of K, we apply the training procedure described previously with increasing values of $\lambda \in \{0.01, 0.015, 0.02, 0.025\}$. We evaluate the resulting models on the test set by computing the effective dimension K' and the deviance of the predicted counts on positive examples. We summarize the model selection results in Figure 5.

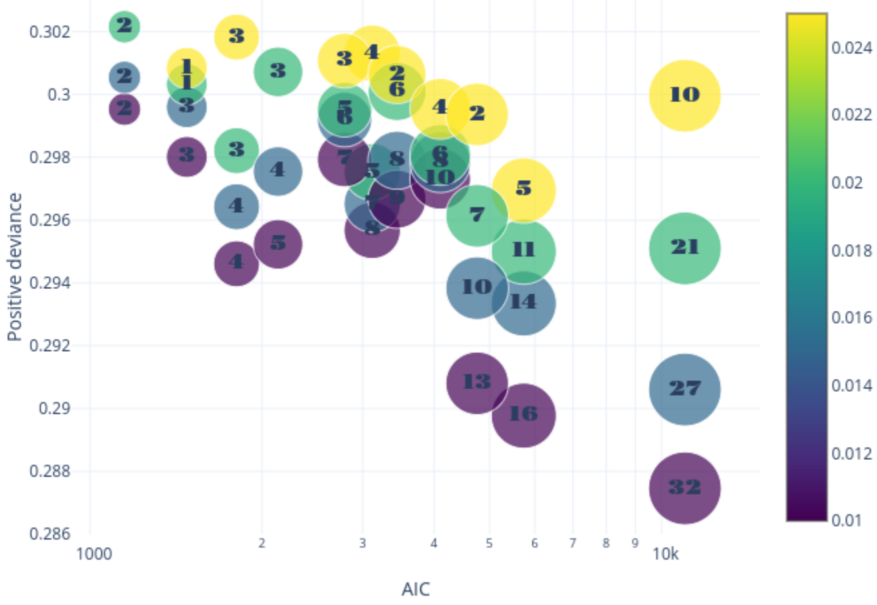

Figure 5: Positive deviance as a function of the Akaike Information Criterion. Each point represented with a circle indicates a configuration of the hyperparameters. Circle size is proportional to embedding size. Circle color represents the value of the lasso penalty parameter λ ranging from 0.01 (darker blueish colors) to 0.03 (brighter yellowish colors). The labels correspond to the number of useful dimensions (non-zero vectors). Larger embeddings lead to a higher model complexity which explains the increasing trend in AIC values with the increase in embedding size. Higher values of λ (yellowish points) induce smaller retained dimensions and larger deviance scores. The combination $(\lambda = 0.01, K = 4)$ provides the best compromise between model complexity and performance. `https://chart-studio.plot.ly/~socco/45`

2.4.5 Analyzing plant associations and their latent representations

In this part, we aim to analyze the inferred associations. We perform a hierarchical clustering on both rows and columns of the association matrix to obtain effect and response groups, displayed in Figure 9a. In parallel, we apply the modularity maximization algorithm on the association network to identify densely connected modules, referred to as communities (Gauzens et al 2015). After that, we map the structural roles to the modules to create the group-level network.

Finally, we investigate the functional determinants of the associations diversity. To do so, we compute the mutual information between the plant traits (Refer to Supplementary materials for full list and documentation) and the learnt representations (Figure 10). The Mutual Information (Shannon and Weaver, 1949; Cover and Thomas, 1991) is an unbounded symmetric and positive score that measures the amount of information contained in one random variable about another. t quantifies the reduction in uncertainty about one random variable given knowledge of another. Zero mutual information indicates independence.

In general, we expect traits related to dispersal capabilities (seed, spread) to affect the prevalence of the species, consequently increasing or decreasing the opportunity to affect other species (interaction probability). As a result, they should be important in the structure of effect embeddings. Conversely, traits related to nutrient uptake and biomass accumulation showcase the competitive or cooperative abilities of the plant species. Hence, we would expect a strong influence on both plants' responses and effects.

3 Results

3.1 Recovering simulated association types

3.1.1 Association classification performances

In average, recall did not vary significantly between positive and negative associations. However, precision was better for the latter. Higher precision was registered for neutral associations. Better performances were reported on smaller datasets with higher recall on dense association configurations against better precision on sparse configurations. Low precision was registered for positive and negative associations indicating presence of spurious associations. The worst performance was obtained for the sparse asymmetric positive simulation.

Association type	Recall %	Precision %	F1-score %
Neutral	60.75	98.64	74.5
Negative	72	34.02	41.23
Positive	77.6	17.6	26.72
Macro-averages	62.45	94.71	73.09

Table 3: Association classification performances.

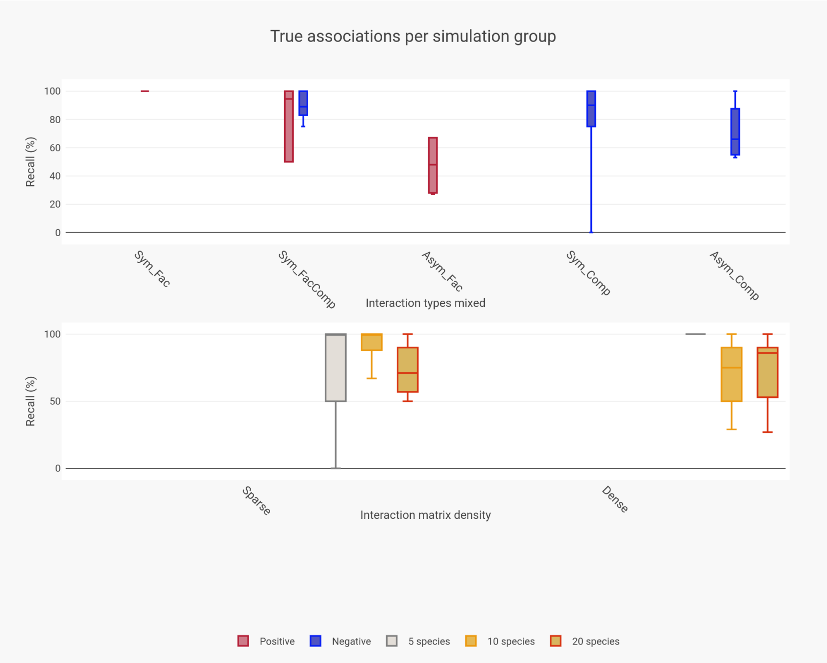

Figure 6: Recall values per simulation groups. `https://chart-studio.plot.ly/~socco/53`

On the other hand, biogeographical filtering increases the recall on neutral associations(more correctly identified non interactions) and the precision of positive and negative associations (less spurious interactions).

3.1.2 Confronting inferred associations to observed patterns

We find that the observed patterns told different stories about the actual associations. The co-occurrence index was higher than 50% for all species with at least one positive effect. However, the species pairs involved in negative associations appeared together more than expected under the independence assumption in some runs and less on others, in particular on bigger pools. Neutral associations induced co-occurrence indices spanning a large spectrum below 70%.

The Geographic Relative Effect on Abundance index (GREA) reflected well the simulated associations with negative (resp. positive) effects below or around (resp. above) zero, while neutral associations were centered around zero. However, most positive effects yielded small values of their respective GREA indices as compared to the negative effects. Although more clearly marked, the latter approached neutrality on bigger and more densely connected communities.

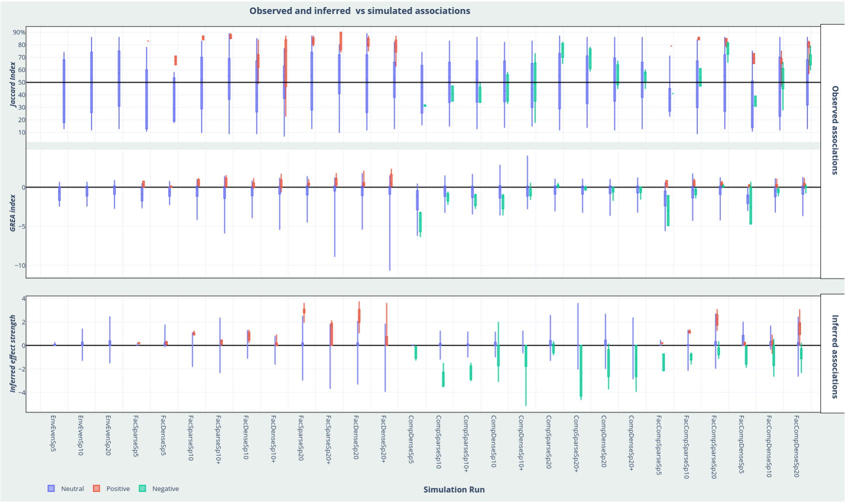

Figure 7: Distribution of co-occurrence, relative abundance effect and inferred association strength per type of association. `https://chart-studio.plot.ly/~socco/30`Interactive mode

The inference model was able to discriminate positive from negative effects while maintaining an average value for non interacting pairs centered on zero. On simulations with a dense mix of positive and negative associations, both observed effects and inferred associations were close to zero, possibly due to opposite effects canceling each other.

3.2 Abiotic and biotic drivers of Alpine plant distributions

3.2.1 Plant habitat suitability

We analyze the parameters and performances of the HSM fitted on plant occurrences. Results are summarized by plant genus groups in Figure 8. The model predicts habitat suitability with at least 70% AUC score for all genuses. The analysis of environmental variable importance shows the dominance of Snow duration followed by zoogenic disturbances, the site form and aspect. Physical disturbance and slope weights were neglectible, probably due to their correlation with Snow.

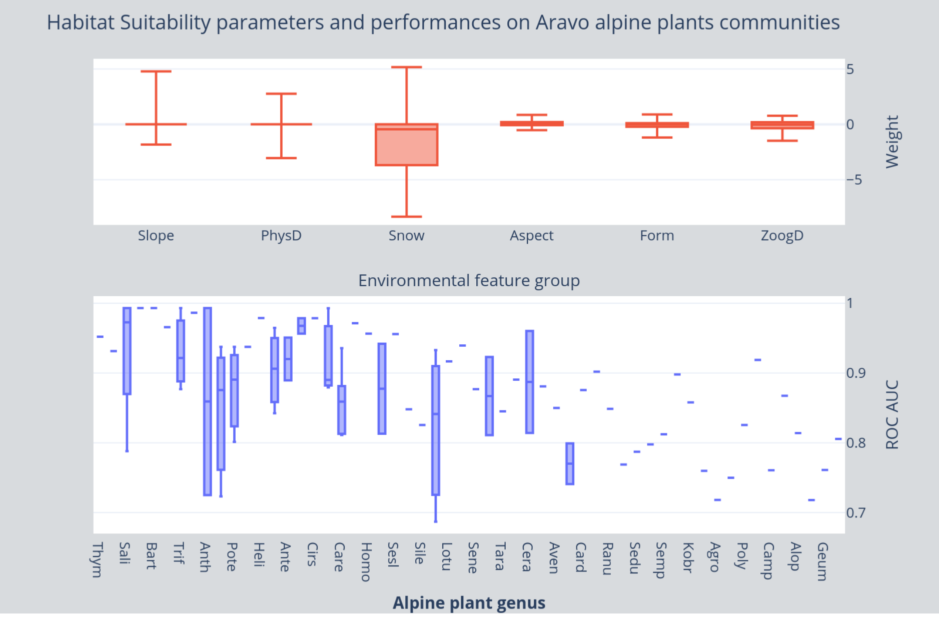

Figure 8: Habitat Suitability Model parameter interpretability and prediction performances.https://chart-studio.plot.ly/~socco/1/

3.2.2 Plant associations on a mesotopographic gradient

We analyze the inferred associations and the overall network structure (Figure 9) in light of existing literature on alpine plants interactions (Choler et al 2001). Four densely connected modules stand out. They are structured along the mesotopographical gradient.

1. High-altitude, dry and windy communities densely connected by positive associations: (i) unselective commensalism of forbs by dominant graminoids, (ii) facilitation between graminoids and tall herbs. The latter act as hubs connecting the high elevation sites to the adjacent sites.

2. Mid-gradient communities composed of two groups: (i) Tall herb grasslands occuring in favorables conditions, mostly structured by negative associations (ammensalism and competition); (ii) Short herb meadows, prone to zoogenic disturbance. They present higher abundances when co-occuring with tall herbs. Through their spreadth they also play a central role in connecting extreme and favorable sites' communities.

3. Chinopholous (cold-resistant) vegetation appearing on late-melting sites. They cohabitate positively with some short-herbs but are negatively affected by forbs and tall herbs.

4. North-facing isolated communities dominated by Salix Herbacea negatively associated with high-altitude communities and characterized by high

eccentricity.

Modules identified on the basis of link density by the modularity maximization algorithm are spatially structured. Hence, the network of modules reflect the spatial connectivity and as a result the turnover over the gradient. Within each commmunity, we identify various subgroups based on different responses (incoming edges) or effects (outgoing edges) to other groups.

For instance, the high-elevation module (pink nodes) comprises three subgroups with different structural roles. Graminoids dominate these communities, they provide wind protection to forbs and some tall herbs (Festucal Violacea, Trifolium Alpinum). The latter also occur on grasslands where they compete with each other. Hence, this subgroup is separated from other forbs despite their cohabitation and the similar response to graminoids.

As reported in the literature (Callaway 2001, Choler 2005), the abiotic stressors strongly structure the distribution of the plant species and the dominant interaction types. Indeed, more positive associations are reported in stressful conditions (high-elevation and late-melting sites). Particularly, the average snow duration seems to be the major structuring force.

3.2.3 Functional meaning of plant embeddings

We analyze in Figure 10 the mutual information of learnt latent representations and plant functional traits. The result show a relatively significant contribution of the Nitrogen mass and Spread to the plants response, whereas the angle was found independent. The Specific Leaf Area contributes significantly to the effect in addition to the Nitrogen mass and on a lesser extent height, spread and seed.

4 Discussion

We first develop a probabilistic model of multispecies abundances that accounts for habitat suitability as well as biotic associations. We parameterize this model with an asymmetric association matrix computed from two sets of low-dimensional embeddings representing: the effect present species have on others' abundance, and the response to other species' effects. We then use the model to infer associations given species abundances.

We use a process-based simulation model to generate synthetic community datasets. By analyzing the observed co-occurrence and pairwise conditional abundances, we note that co-occurrence levels can be high even on known competing pairs if the species pool is small and the communities' carrying capacity is large. On the other hand, the abundance reflects better the nature of associations as it is lower than average in presence of negative associations and higher with positive associates. Nonetheless, pairwise abundance effects may turn out to be neutral in presence of multiple confounding effects (Boulangeat et al 2012). Consequently, one should model the pairwise associations conditioned on all other species in order to isolate the different opposing influences. For instance, given a triplet A, B, C such that A (resp. C) influences B positively (resp. negatively). If the same strength is applied by A and B we may observe that all pairs are independent, unless we evaluate the association $A->B$ conditioned on C and $C->B$ conditioned on A. In any case, we still need separate observations where we could quantify both associations separately.

Thereafter, we test the ability of the model to recover simulated associations. We find that the model is able to disentange positive, negative and neutral associations. But, it generates many spurious associations due to high levels of co-occurrence induced by the simulation model. As opposed to Joint Species Distribution Models, our model is able to recover positive associations between species with similar abiotic niches, for two reasons. First, it does not rely on residuals unexplained by the SDM. Instead, it conditions on the habitat suitability for both species hence the probability of them co-occurring would induce a potential for facilitation. Second, the association is evaluated on the basis of abundance variation in presence of the other species.

Afterwards, we apply the inference model on plants distributed along a mesotopographical gradient in the French Alps. The associations identified by the algorithm conformed to most of the important specific relationships that we expect to find in the upland plant community (Choler 2001), giving us confidence in the novel methods presented here. We observe more positive associations in extreme conditions (dry, windy or frozen) and negative ones in favorable sites, confirming the stress-gradient hypothesis (Callaway et al 2007). We illustrate using the results on Aravo dataset some of the possibilities allowed by the model. For instance, we can use the association matrix to populate a network, study its modular structure through community detection algorithms and analyze the structural roles, including effect and response groups, occupied by species within communities. Such information is useful to evaluate the functional redundancy within communities. Second, we argue that the learnt representations can be related to functional traits of the species, providing the appropriate traits are measured, to identify the functional drivers of network structure.

It is now agreed upon that inferred associations are not biological interactions. They represent significant spatial colocation or dislocation patterns, that are informative in a predictive rather than causal way (Mils et al 2012). The specific mechanism that led to these patterns may vary from pair to pair, ranging from direct interactions (e.g trophic), to indirect interactions (e.g engineering).

The problem of inferring associations from co-occurrence is a major part of ecological modeling publications, as much as biomedical and bioinformatics literature. Existing approaches include JSDMs (Ovaskainen et al 2017) which rely on explaining residual correlations by biotic effects but cannot by design model asymmetric associations. Other major state of art methods are based on probabilistic graphical models including Markov Random Fields (Harris et al 2015, Chiquet al 2017) and Bayesian networks (Mils, Trifonova, Aderhold et al 2012). The former yields undirected networks while the latter impose a directed acyclic structure to the network of associations forbiding feedbacks and the modeling of asymetric effects.

The most challenging part of this task is that it is completely unsupervised, with no prior or guidance on the expected associations or network. Hence, validating the resulting associations is tricky. It is still feasible to evaluate the veracity of the type of associations by using an edge classification scheme and a list of potential interactions as we've shown. However, it is far more difficult to validate the strength of associations especially when working with snapshot data. As many associations would have a strength around zero, it is also valuable to ask whether one should use higher thresholds to decrease the amount of spurious associations and increase model precision and how to select these thresholds ? Moreover, because many processes influence community assembly, multiple scenarios could lead to the same communities making this problem unidentifiable. In this case, we need not one expected list of associations but all the possible ones or a goodness-of-fit measure that accounts for equivalence between different association combinations.

A possible way to prevent the unidentifiability issue is to include known information on ecological interactions in the model (Cazelles et al 2015). For instance, (Staniczenko et al 2017) use a Bayesian network with a structure defined a priori, and trains its parameters using an SDM to predict species occurrence probabilities. In our case, such constraints can be defined by altering the biotic context definition. One direct way to do it is to consider a customized biotic context for each species composed of the set of its potential interaction partners in a regional metaweb.

There is now growing evidence that ecological interactions are context-dependent (Poisot et al 2012, Tikhonov et al 2017), we show in appendix B how to infer associations whose strength is modulated by other covariates (e.g: stress, presence of predator, etc.) Recently developed models account for association variability as a function of the environmental context (Tikhonov et al 2017, Clark et al in prep). Despite the new possibilities offered by these developments, the question of how to validate their results still araises itself.

Finally, although the main purpose of the model is to infer species associations, it is also useful to make conditional predictions of abundances. Another possible usage is to perform link prediction on an incomplete network. The idea is to complete the associations involving a target species by leveraging information from similar node species.

5 Conclusion

Biological interactions and other processes induce spatial patterns of co-occurrence. Our objective is to disentangle these processes and isolate species dependencies. We present a model of species co-abundances as a function of the habitat and biotic associations. We propose an asymetric scheme for modeling associations that is based on learning latent representations of species responses and effects. Future efforts should be directed towards a combination of prior knowledge on the complete or partial topology of the association networks to guide the inference process. Along with that, a strong theory of how known ecological interactions influence the co-distribution of species is needed to support all these models.

A Derivatives of the optimized objective

Canonic derivatives (refer to Liping liu et al 2017).

B Alternative biotic context definitions

B.1 Associations that depend on external factors

In the base model, the outcome of any pairwise interaction is invariant with respect to the abiotic or biotic conditions surrounding it. To account for that, we introduce a slight alteration to the vanilla model where we allow the embeddings of the biotic context to depend on some chosen variables. We stack the latter in a vector of p covariates noted V, such that V_{ij} denotes the value of the j^{th} covariate on the i^{th} site.

Given an embedding dimension of d latent variables, we start by computing the weight attributed to each dimension as a regression function g, with a parameter vector γ, over the conditioning covariates.

$$g : \mathbb{R}^p \mapsto \mathbb{R}^d$$

$$\beta_i = g(V_i; \gamma)$$

For instance, we could set:

$$g : V \mapsto \gamma \cdot V + 1_d$$

In which case:

$$\beta_i = \textstyle\sum_{l=1}^{d} \gamma_l \cdot z_{i,l} + 1$$

The resulting biotic context can be embedded as follow, where $*$ is the elementwise vector product:

$$z_{i,j} = \beta_i * (\frac{1}{|c_{i,j}|} \sum_{k \in c_{i,j}} y_{i,k} \alpha_k) = \frac{1}{|c_{i,j}|} \sum_{k \in c_{i,j}} y_{i,k} (\beta_i * \alpha_k)$$

Recovering the biotic associations: We proceed similarly to the vanilla model by isolating the pairwise interactions on the response variable. In this case, instead of a 2D matrix, the associations we obtain are retrieved in a three-dimensional tensor $\mathcal{A}$. Each slice on the first dimension of $\mathcal{A}$ represents a local association network.

$$\mathcal{A}_{i,j,k} = \sum_{l=1}^{d} \beta_{il} \cdot \rho_{jl} \cdot \alpha_{kl}$$

$$\eta_{i,j} = f(\frac{1}{|c_{i,j}|} \sum_{k \in c_{i,j}} y_{i,k} \mathcal{A}_{i,j,k} + o_j)$$

By incorporating the environmental covariates on the latent space, we gain two desirable properties. First, we get a fixed number of parameters that is a factor of the embedding dimension, which is significantly smaller than the number of modeled taxa. Second, we ensure taxa with similar latent traits, willingly captured by the response and effect embeddings, share associations regardless of the surrounding conditions. As a result, response or effect groups of taxa computed from the learnt embeddings remain consistent in the environmental space.

B.2 Temporal model

When time-series are available, we model the target variable $y_{ij}^{(t)}$ denoting the abundance of a taxa T_j, on a location S_i, at a certain time t. We do that by simply changing the **biotic context** definition to: *the set of taxa, including the target, that were observed in the previous timestamp.*

$$c_{i,j}^{(t)} = \{k \mid y_{i,k}^{(t-1)} > 0\}$$

$$z_{i,j} = \frac{1}{|c_{i,j}^{(t)}|} \sum_{k \in c_{i,j}^{(t)}} y_{i,k}^{(t-1)} \cdot \alpha_k$$

B.3 Spatial model

Given a distance measure δ and a radius r, we consider a spatial extension of the model where the **biotic context** is defined as : *the set of taxa that were observed at a significatively close location.*

$$c_{i,j} = \{(s,k) \mid \delta(S_i, S_s) \leq r \ , \ y_{s,k} > 0\}$$

One can use multiple radius values customized to the dispersal abilities of each target group or taxa for instance. The effect of each contextual element is subdued by its distance to the target location. The hyperparameter τ controls the decrease in importance per unit of distance. Similarly, τ can be customized for each group of taxa by expert knowledge.

$$z_{i,j} = \textstyle\sum_{(s,k)\in C_{i,j}} y_{s,k} \cdot \alpha_k \cdot \exp^{(-\delta(S_i,S_s)\tau)}$$

B.4 Graph biotic context

So far, we defined the biotic context using the community composition in terms of taxa and eventually their abundances. At this point, we are able to capture pairwise additive effects. However, we miss the impact of interactions between context taxa or the whole network structure around the target location on the abundance distribution of the target group.

Fortunately, graph embedding algorithms permit the incorporation of structured data such as knowledge graphs into predictive models. For instance, we can define the **biotic context** as the interaction network at the focal point S_i minus the target taxa T_j, noted $\mathcal{G}_{i/j}$. The **context embedding** is obtained by applying a graph kernel function $\mathcal{K}$ with parameter α on the contextual network.

$$z_{i,j} = \mathcal{K}(\mathcal{G}_{i/j}; \alpha)$$

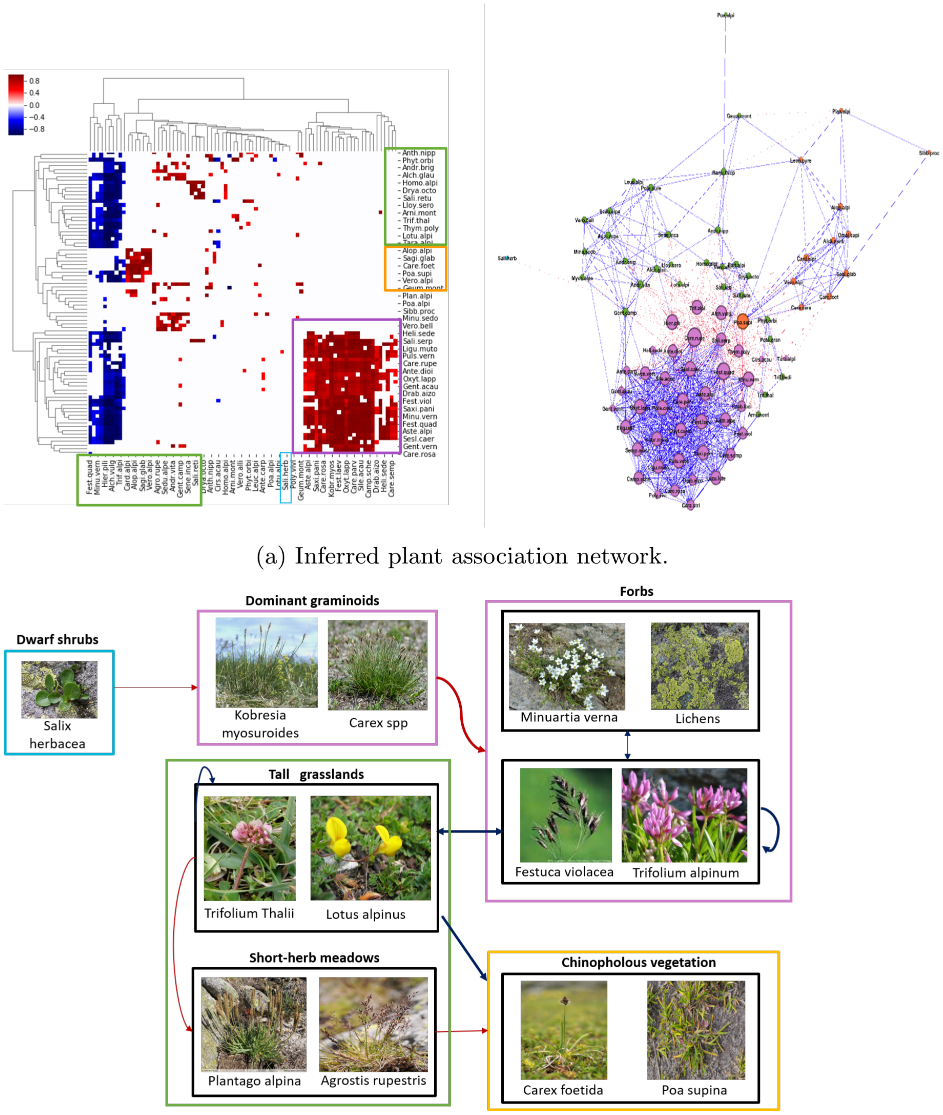

(a) Inferred plant association network.

(b) Summary network of plant associations.

Figure 9: Plant associations on an alpine mesotopographic gradient. Subfigure (a) shows the normalized pairwise associations on the left and the corresponding network on the right. Blue (resp. red) edges indicate negative (resp. positive) edge weights. Node colors on the graph represent communities identified by the modularity maximization algorithm (Newman et al 2006). We highlight the communities composition using colored squares on the matrix on the right. Species in the association matrix are grouped based on a hierarchical clusterings performed rowise (yielding response groups) and columnwise (yielding effect groups). Subfigure (b) summarizes the association network at the level of previously identified groups. Edge thickness is proportional to the number of links between the interacting group pair.

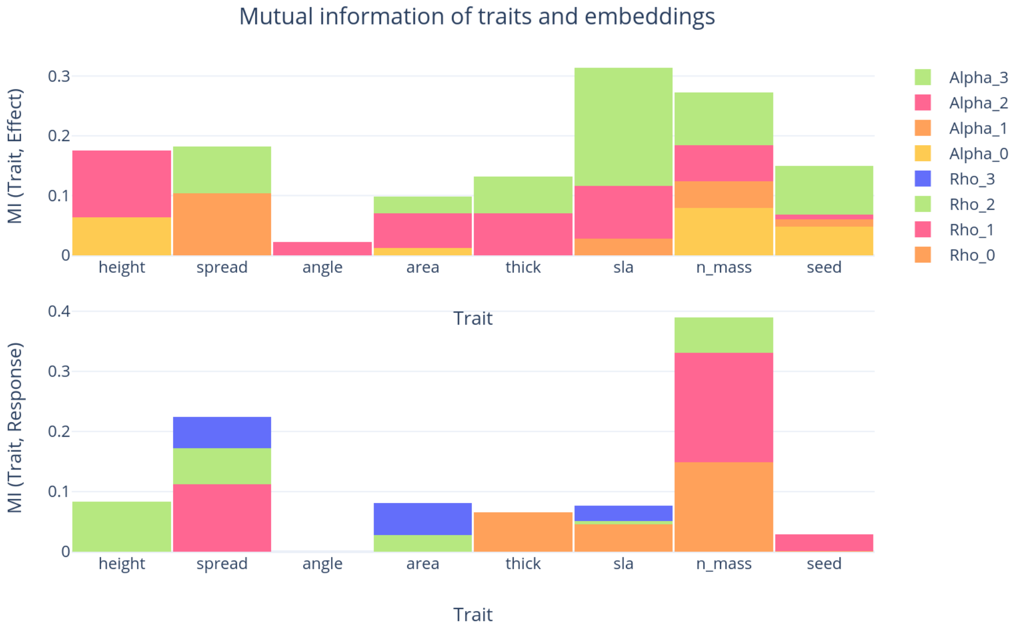

Figure 10: Mutual information between plant traits and their latent representations. Each bar concerns a specific trait, it represents the stack of mutual information scores from the first to the last (fourth) embedding dimension. The lower (resp. upper) figure shows the results for the response (resp. effect) embeddings. `https://chart-studio.plot.ly/~socco/70`